Change of the Fermi surface of Gd metal upon magnetic ordering as seen via angle-resolved photoelectron spectroscopy

K. M. Döbrich,[1,2] A. Bostwick,[3] E. Rotenberg,[3] and G. Kaindl[1]
[1]*Institut für Experimentalphysik, Freie Universität Berlin, Arnimallee 14, 14195 Berlin, Germany*
[2]*Max-Born-Institut, Max-Born-Straße 2a, 12489 Berlin, Germany*
[3]*Advanced Light Source, Lawrence Berkeley National Laboratory, Berkeley, California 94720, USA*
(Received 2 December 2009; published 12 January 2010)

Fermi surface and valence-band structure of Gd metal were studied in a complete Brillouin zone by angle-resolved photoelectron spectroscopy in both the paramagnetic and the ferromagnetic phases, revealing substantial changes upon magnetic ordering. These comprehensive experimental Fermi-surface data represent a reference for various theoretical results and are essential for an improved understanding of the origin of magnetic ordering in lanthanide metals.

DOI: 10.1103/PhysRevB.81.012401 PACS number(s): 75.50.Cc, 71.18.+y, 71.20.Eh, 79.60.−i

The electronic states at the Fermi energy (E_F) of a metal, which form the Fermi surface (FS) in k space, determine its macroscopic low-energy excitation properties, such as electrical conductivity, heat capacity, and optical properties. For the magnetic lanthanide (Ln) metals, their role is even more important since the conduction electrons at E_F are known to mediate the coupling between the localized $4f$ moments (Ruderman-Kittel-Kasuya-Yoshida, RKKY, interaction) and the shape of the FS determines the development of various types of long-range magnetically ordered phases.[1–3] In a few cases, theoretical results are available that predict changes of the FS and of valence-band states upon magnetic ordering. For Gd metal, calculations of the electronic band structure (BS) along specific high-symmetry lines of the Brillouin zone (BZ) have been reported.[4–6] The experimental situation with respect to FS of Ln metals and their changes upon magnetic ordering, however, is still quite unsatisfactory. Previous photoemission (PE) studies of Gd metal focused on specific aspects of the electronic structure, e.g., the positions of band states at high-symmetry points or specific symmetry lines of the BZ,[7] as well as the temperature dependence of the magnetic exchange splitting of specific bands (bulk and surface), again at certain positions in k space.[8–14] In the case of Gd metal, the FS had previously been studied experimentally in the paramagnetic (PM) phase by positron annihilation,[15] while in the ferromagnetic (FM) phase, de-Haas-van-Alphen (dHvA) frequencies for certain extremal orbits had been reported and compared with theoretical results.[16]

In this Brief Report, we present a comprehensive angle-resolved photoelectron spectroscopy (ARPES) study of the FS and the valence BS of Gd metal. Data are presented for the valence bands along several high-symmetry lines of the hexagonal BZ of Gd metal, i.e., parallel to the surface of the (0001)-oriented sample, and cuts of its FS with high-symmetry planes of the BZ are shown. We focus in particular on differences between the PM and the FM phases that are shown to originate mainly from magnetic exchange splitting ΔE_{ex} of bands in the FM phase. The derived FS maps provide a comprehensive experimental picture of the BS of Gd metal and reveal the effects of FM ordering on the FS within a complete BZ. Furthermore, we compare the experimental data with the results of various theoretical approaches and point out remaining discrepancies.

The measurements were performed at beamline 7.0.1 of the Advanced Light Source, Lawrence Berkeley National Laboratory, on 10-nm-thick Gd films grown *in situ* on W(110). Photon energies from 85 to 110 eV were employed giving access to the Δ_2-like bands.[17] The FS data were derived from a series of angle-resolved maps of PE intensities at various photon energies and emission angles. Data sets were recorded both at room temperature, where Gd is PM, and at 50 K, where Gd is FM (Curie temperature T_C=293 K). At 50 K, ΔE_{ex} amounts already to almost the full ground-state splitting.[11]

Figure 1 displays measured electronic bands along the ΓM, MK, and ΓK high-symmetry directions for (b) the PM and (c) the FM phase, respectively; the hexagonal BZ is shown in (a). For the ΓM section, e.g., k_x and k_z are kept constant and the PE intensity, proportional to the darkness of the gray tones, is plotted versus k_y and $(E-E_F)$. In (b), two bands are readily identified, with one of them fully occupied (thick line) crossing the Γ point at $(E-E_F)=-1.87\pm0.03$ eV. In ΓK direction, this band comes close to E_F, but does not cross. A second band, unoccupied at Γ (thin line), crosses E_F twice, at positions labeled 1 in ΓM and 2 in ΓK direction, with $k_\parallel$ components of the Fermi vectors amounting to 0.31 and 0.36 Å^{-1}, respectively. Fermi vectors were determined as described in Ref. 17, yielding experimental error bars of ±0.03 Å^{-1}. The band forms a holelike feature of the FS. In our previous study of Tb metal,[17] with its related electronic structure, the former band has been identified as band 2 and the latter one as band 3. In the FM phase (c), the bands are exchange split, with the majority (↑) and minority (↓) components at Γ at $(E-E_F)=-2.26\pm0.03$ and -1.37 ± 0.03 eV, respectively. This results in ΔE_{ex}=0.9 eV (fit analyses are not shown here), in very good agreement with the results of earlier PE studies.[8,12,14] The majority band 2↑ has a lower PE peak intensity than the minority component 2↓, caused by increased lifetime broadening in case of the deeper photo hole. In the FM phase, band 2↓ (thick dashed line) crosses E_F close to the K point (at 3′, $k_\parallel$=1.15 Å^{-1}) and on the ΓK line (at 4′, $k_\parallel$=0.70 Å^{-1}), resulting in a new FS feature, while band 2↑ (thick solid line) moves away from the Fermi level. Magnetic exchange splitting is also observed for band 3,

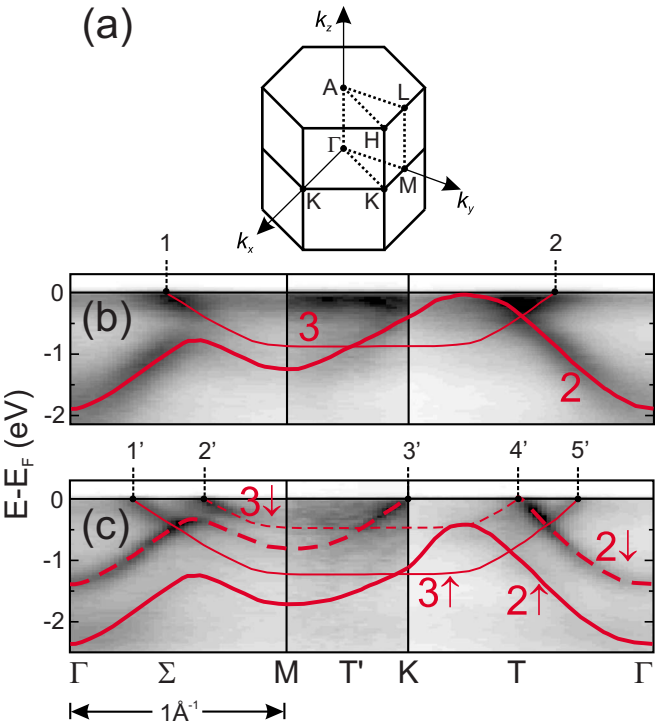

FIG. 1. (Color online) (a) BZ of Gd metal with high-symmetry points and directions in k space; the wedge spanned by the dotted lines marks the irreducible part of the BZ. (b) Observed PE intensity from Gd metal in the PM phase at 300 K as a function of $(E-E_F)$ along the ΓM, MK, and ΓK high-symmetry directions (k_z=5.24 Å^{-1}, $h\nu$=105–110 eV); (c) same in the FM phase at 50 K. Lines serve as a guide to the eyes and highlight the dispersions of band 2 (thick) and band 3 (thin); band crossings with E_F are numbered. In the FM phase, the bands are exchange split in majority (solid) and minority (dashed) states.

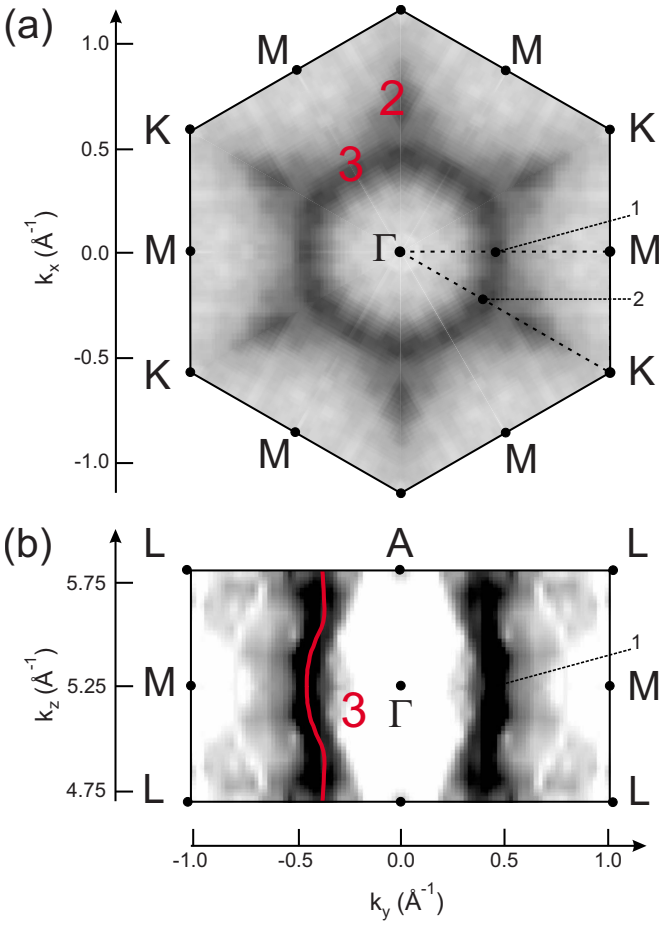

FIG. 2. (Color online) Fermi contours of Gd metal in the PM phase at 300 K: (a) in the ΓMK plane, i.e., parallel to the sample surface, measured at photon energies from 105 eV at Γ to 110 eV at M. Band 3 forms a Γ-centered ring (hole pocket). In ΓK direction, high PE intensity is observed, when band 2 comes close to E_F. (b) The cut perpendicular to the sample surface in the ΓALM plane reveals a ring-shaped feature that disperses toward the zone boundary with varying diameter; the line on the left follows the dispersion as a guide to the eyes (photon energies from 85 eV at A to 110 eV at M).

where the majority and minority parts cross E_F at the locations 1′, 5′ and 2′, 4′, at $k_\parallel$ of 0.28, 0.40, 0.60, and 0.70 Å^{-1}, respectively. The calculated BS for ΓM, MK, and ΓK, presented in Refs. 5 and 6, are in good agreement with our experimental results; details, however, are at variance: In Ref. 5, the bands are too low in energy relative to E_F, an effect that is stronger for the majority bands. The calculated ΔE_{ex} is also overestimated by ≈100 meV, depending on the specific band and the position in k space. These findings are similar to what has been reported for Tb.[17] In Ref. 6, the agreement with the experimental data is better for the majority states than for the minority states, and generally for states closer to E_F; these drawbacks of the calculated BS may be caused by hybridization with unoccupied 4f states. On the other hand, earlier theoretical results[16] are at much greater variance with the experiment.

The Fermi contours in the ΓMK plane are obtained by plotting the PE intensities at E_F for constant k_z. We first discuss the PM phase [see Fig. 2(a)], where a ring-shaped contour centered at Γ is observed (note that the data are mirrored along the high-symmetry lines of the hexagonal BZ; for details, see further below).

Increased PE intensities occur also in the middle of the ΓK line, due to finite experimental resolution and phonon broadening, when band 2 approaches E_F [see Fig. 1(b)]. The hexagonal sixfold rotational symmetry around Γ is clearly visible. The dashed triangle spanned by Γ, M, and K follows the bandmap shown in Fig. 1(b), including the numbered crossings of the bands with E_F. In order to follow the Fermi contours perpendicular to the sample surface on the ΓLM plane, we plot the PE intensities $I(k_y,k_z)$ at E_F for k_x=constant in Fig. 2(b). The ring-shaped FS feature in the ΓMK plane, which is formed by band 3, continues toward the AL zone boundary with varying diameters, showing its maximum in the ΓMK plane.

In the FM phase (Fig. 3), the FS changes quite dramatically due to magnetic exchange splitting of the bands, causing the majority and minority Fermi contours to separate, as shown for the ΓMK plane in Fig. 3(a). While the 3↑ contour shrinks with increasing ΔE_{ex} and moves toward Γ, the 3↓ contour grows and turns hexagonal when coming closer to the zone boundary. The observed behavior follows a general

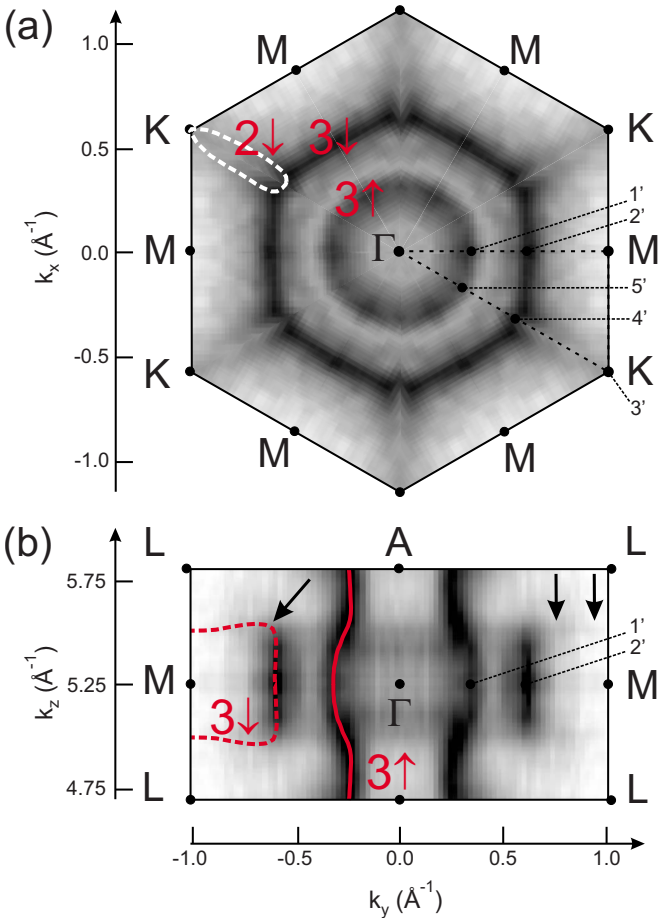

FIG. 3. (Color online). Fermi contours of Gd metal in the FM phase at 50 K: (a) in the ΓMK plane; (b) in the ΓLM plane. Magnetic exchange splitting causes the electronic states to separate, which induces significant changes of the FS. The lines follow the Fermi contours and serve as a guide to the eyes.

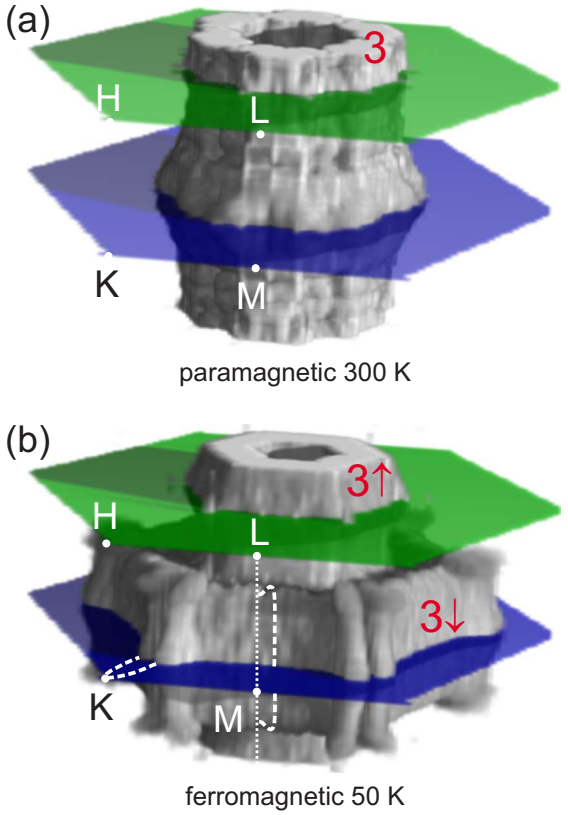

FIG. 4. (Color online). Fermi surface of Gd metal, covering a complete BZ: (a) PM phase, where band 3 forms a central pillarlike structure; (b) FM phase, where minority and majority Fermi-surface sheets are separated due to exchange splitting. Dashed lines indicate the dispersion of the Fermi contours according to Figs. 3(a) and 3(b) in the region close to the MKHL zone boundary, where PE intensities of the Fermi contours are too weak to be seen in the three-dimensional plots.

tendency: majority hole pockets of the FS shrink and move closer to their center with increasing ΔE_{ex}, while minority hole pockets grow and move away from their center (electron pockets behave oppositely). As already seen in Fig. 1(c), band 2↓ now crosses E_F, resulting in an elliptically shaped FS feature with low PE intensity that is marked by the white dashed line; it starts at the K point and extends halfway to the Γ point. Again, the numbering of the band crossings with E_F follows the band map in Fig. 1(c) (data mirrored as in Fig. 2). In the ΓLM plane [Fig. 3(b)], the exchange splitting of the bands leads also to significant changes of the FS; the band-3↑ contour has a smaller diameter as compared to the PM phase in Fig. 2(b) and lies closer to the ΓA line. Consequently, it reaches the zone boundary close to the A point. Band 3↓ is observed with high PE intensities in the middle of the ΓM line. It shows a straight dispersion in k_z direction (i.e., toward the AL zone boundary) and turns toward the ML line at the position marked by an arrow. At the kink, the PE intensity drops significantly. The 3↓ contour can be traced toward the zone boundary with very low intensity, slightly above background level (see raw data marked by vertical arrows on the right the side of the figure). It reaches the zone boundary at about halfway on the ML line. This behavior is similar to previous observations for Tb metal.[17] The calculations in Ref. 16 show good agreement for bands 3↑ and 3↓ in the ΓMK plane (note that these bands were labeled 5↓ and 7↑, respectively, in Ref. 16), however the feature stemming from band 2↓ is missing. In the ΓALM azimuth, the calculated band 3↑ reaches the AL zone boundary too close to the L point, and the dispersion of band 3↓ deviates significantly from the experimental data.

In order to provide a comprehensive picture of the FS of Gd metal, we plot $I(k_x,k_y,k_z)$ for $E=E_F$. This requires a uniform normalization of the PE intensities throughout the BZ.[20] A mirroring procedure, exploiting the hexagonal symmetry, was applied to overcome this problem. To this end a special numerical routine was developed: First, the irreducible part of the BZ was picked at a given k_z, starting on the ΓMK plane, where the irreducible part is the area of the triangle spanned by Γ, M, and K [marked by dashed lines in Figs. 2(a) and 3(a)]. In a second step, hexagonal rotational and mirror symmetries were applied, and the data were duplicated several times, to cover the full hexagon of the BZ in the ΓMK plane. The PE intensities at const. k_z were normalized to the range of 0 to 1 by setting the lowest observed intensity to 0 (background level) and the highest intensity to 1 (brightest Fermi contour), using a linear scale for interme-

diate PE intensities. This symmetrization and normalization procedure was repeated for all planes parallel to ΓMK, leading in this way to a uniform normalization of PE intensities (see also Ref. 18).

The results of this data treatment are shown in Fig. 4, where the FS formed by band 3 in a range comprising a complete BZ, is displayed. In (a), the pillarlike structure of the FS of Gd in the PM phase is displayed, with its maximum diameter in the ΓMK plane. These results are in very good qualitative agreement with the FS obtained by positron annihilation[15] (note that the FS of Gd shown in Ref. 15 is cut along ΓMK). Temperature-dependent studies of the FS have not been reported by positron annihilation, however, due to very long data-acquisition times of up to several months.[19] With ARPES, a comparable data set can be recorded within 3 to 4 h, providing experimental access to changes of the FS induced by magnetic ordering. In Fig. 4(b) the FS of Gd metal in the FM phase is shown. The central pillarlike structure, formed by majority states, has a smaller diameter than in the PM phase, according to the general behavior of hole pockets discussed above. The minority states form a hexagon that is separated from and surrounds the central structure. The sections of the 3↓ feature that disperse parallel to the ΓMK plane cannot be seen in the plot due to very low PE intensities in the region close to the MKL zone boundary. The dashed line close to the ML line (dotted) reflects the dispersion on the ΓLM azimuth, as shown in Fig. 3(b). Due to low PE intensity, only the innermost part of the band-2↓ contour is visible, manifesting itself as an extension parallel to the KH line at the corners of the 3↓ hexagon. Its dispersion in the ΓMK plane, see Fig. 3(a), is marked by the dashed line close to K.

In summary, we have presented a comprehensive study of the electronic properties of the heavy Ln metal Gd, covering a broad temperature range and a wide region in k space. ARPES provides direct access to the shape of the FS, with no need for theoretical input, as it is the case with dHvA measurements that are limited to bulk crystals and the FM phase at low temperatures. Our FS data for the PM phase are in agreement with previous results of positron-annihilation studies. A comparison of results from various theoretical approaches with the present experimental data reveals discrepancies, such as an overestimation of ΔE_{ex} as well as differences in the dispersions of bands and in Fermi contours. The present results serve as an experimental reference and are expected to play a role in improving future theoretical models as well as the understanding of the magnetic ordering in Ln metals.

The authors acknowledge contributions by Kai Starke (deceased) in the early stages of this work. This work was supported by the Deutsche Forschungsgemeinschaft, Project No. STA 413/3-1, the German Bundesminister für Bildung und Forschung, Project No. 05 KS1KEC/2, and the U.S. Department of Energy under Contract No. DEAC03-76SF00098.

[1] I. D. Hughes, M. Däne, A. Ernst, W. Hergert, M. Lüders, J. Poulter, J. B. Staunton, A. Svane, Z. Szotek, and W. M. Temmerman, Nature (London) **446**, 650 (2007).
[2] A. J. Freeman, in *Magnetic Properties of Rare Earth Metals*, edited by R. J. Elliott (Plenum Press, London, 1972).
[3] J. Jensen and A. R. Mackintosh, *Rare Earth Magnetism* (Clarendon, Oxford, 1991).
[4] J. O. Dimmock and A. J. Freeman, Phys. Rev. Lett. **13**, 750 (1964).
[5] P. Kurz, G. Bihlmayer, and S. Blügel, J. Phys.: Condens. Matter **14**, 6353 (2002).
[6] C. Santos, W. Nolting, and V. Eyert, Phys. Rev. B **69**, 214412 (2004).
[7] F. J. Himpsel and B. Reihl, Phys. Rev. B **28**, 574 (1983).
[8] B. Kim, A. B. Andrews, J. L. Erskine, K. J. Kim, and B. N. Harmon, Phys. Rev. Lett. **68**, 1931 (1992).
[9] D. Li, J. Zhang, P. A. Dowben, and M. Onellion, Phys. Rev. B **45**, 7272 (1992).
[10] E. Weschke, C. Schüßler-Langeheine, R. Meier, A. V. Fedorov, K. Starke, F. Hübinger, and G. Kaindl, Phys. Rev. Lett. **77**, 3415 (1996).
[11] C. Schüßler-Langeheine, E. Weschke, C. Mazumdar, R. Meier, A. Y. Grigoriev, G. Kaindl, C. Sutter, D. Abernathy, G. Grübel, and M. Richter, Phys. Rev. Lett. **84**, 5624 (2000).
[12] E. Weschke and G. Kaindl, J. Phys.: Condens. Matter **13**, 11133 (2001).
[13] K. Maiti, M. C. Malagoli, E. Magnano, A. Dallmeyer, and C. Carbone, Phys. Rev. Lett. **86**, 2846 (2001).
[14] K. Maiti, M. C. Malagoli, A. Dallmeyer, and C. Carbone, Phys. Rev. Lett. **88**, 167205 (2002).
[15] H. M. Fretwell, S. B. Dugdale, M. A. Alam, D. C. R. Hedley, A. Rodriguez-Gonzalez, and S. B. Palmer, Phys. Rev. Lett. **82**, 3867 (1999).
[16] R. Ahuja, S. Auluck, B. Johansson, and M. S. S. Brooks, Phys. Rev. B **50**, 5147 (1994).
[17] K. M. Döbrich, G. Bihlmayer, K. Starke, J. E. Prieto, K. Rossnagel, H. Koh, E. Rotenberg, S. Blügel, and G. Kaindl, Phys. Rev. B **76**, 035123 (2007).
[18] K. M. Döbrich, Ph.D. thesis, Freie Universität Berlin, 2008.
[19] S. J. Crowe, S. B. Dugdale, Zs. Major, M. A. Alam, J. A. Duffy, and S. B. Palmer, Europhys. Lett. **65**, 235 (2004).
[20] The present measurements with different photon energies and at different angles at equivalent points of the BZ yield the same Fermi contours (not shown here), however, with different PE intensities, due to changes in the PE cross section. Symmetrization successfully suppresses such intensity variations for presentation.